

This article was downloaded by: [Siauliu University Library]

On: 17 February 2013, At: 00:31

Publisher: Taylor & Francis

Informa Ltd Registered in England and Wales Registered Number: 1072954 Registered office: Mortimer House, 37-41 Mortimer Street, London W1T 3JH, UK



Molecular Crystals and Liquid Crystals

Publication details, including instructions for authors and subscription information:

<http://www.tandfonline.com/loi/gmcl20>

Local Dynamics of Director Reorientation under Electric Field in Helical LC Structure

A. A. Karetnikov^a, N. A. Karetnikov^a, A. P. Kovshik^a, E. I.

Rjuntsev^a, E. V. Aksenova^a, E. V. Kryukov^a & V. P. Romanov^a

^a St. Petersburg State University, Physics Department, Ulyanovskaya St., 1, Petrodvorets, St. Petersburg, 198504, Russia

Version of record first published: 13 Jun 2012.

To cite this article: A. A. Karetnikov, N. A. Karetnikov, A. P. Kovshik, E. I. Rjuntsev, E. V. Aksenova, E. V. Kryukov & V. P. Romanov (2012): Local Dynamics of Director Reorientation under Electric Field in Helical LC Structure, *Molecular Crystals and Liquid Crystals*, 561:1, 97-106

To link to this article: <http://dx.doi.org/10.1080/15421406.2012.687140>

PLEASE SCROLL DOWN FOR ARTICLE

Full terms and conditions of use: <http://www.tandfonline.com/page/terms-and-conditions>

This article may be used for research, teaching, and private study purposes. Any substantial or systematic reproduction, redistribution, reselling, loan, sub-licensing, systematic supply, or distribution in any form to anyone is expressly forbidden.

The publisher does not give any warranty express or implied or make any representation that the contents will be complete or accurate or up to date. The accuracy of any instructions, formulae, and drug doses should be independently verified with primary sources. The publisher shall not be liable for any loss, actions, claims, proceedings, demand, or costs or damages whatsoever or howsoever caused arising directly or indirectly in connection with or arising out of the use of this material.

Local Dynamics of Director Reorientation under Electric Field in Helical LC Structure

A. A. KARETNIKOV, N. A. KARETNIKOV, A. P. KOVSHIK,
E. I. RJUMTSEV, E. V. AKSENOVA,* E. V. KRYUKOV,
AND V. P. ROMANOV

St. Petersburg State University, Physics Department, Ulyanovskaya St., 1,
Petrodvorets, St. Petersburg, 198504, Russia

The influence of an electric field on the trajectory of an extraordinary light ray in a layer of a chiral liquid crystal (LC) with a 180° turn of the director is studied. In the absence of the electric field and at a large angle of incidence the ray reflects inside the layer and return back through the surface which it entered. The applied electric field distorts the initial configuration of the director. It results in a change of the ray trajectory so that the light is propagated through the LC cell. The study of the temporal characteristics of the effect at various angles of incidence of light on the layer makes it possible to examine the local reorientation of the director inside the cell.

Keywords helical liquid crystal; Freedericksz transition; optical response

PACS 42.70.Df; 42.25.Bs; 42.25.Fx; 42.25.Gy

1 Introduction

The study of light propagation in chiral systems in external fields is of special interest in investigation of the optical properties of liquid crystals (LC). For the first time this problem was considered by Freedericksz and Zwetkoff. They studied the propagation of light in a planar oriented layer of a nematic liquid crystal with a 180° super-twist structure in external magnetic field. Reflection of an extraordinary light ray inside the layer at the incidence angles exceeding the angle of total internal reflection of an ordinary ray was discovered [1]. The refraction of the extraordinary ray inside an LC layer was also studied in the layers with different director profiles [2–7]. In our works [8–10], we studied propagation of the extraordinary ray in a 180° helical LC structure experimentally and theoretically. In Ref. [9] it was studied the dependence of the distance from the boundary where the extraordinary ray was reflected as a function of the angle of incidence. In Ref. [10], the effect of the electric field directed along the axis of the helix on the trajectory of the extraordinary ray was studied. In the absence of electric field the angle of the extraordinary ray incidence on the liquid crystal was chosen so that the ray refracted in the middle of the layer. When the external field is applied normal to the cell plane the configuration of the director in the cell

*Address correspondence to E. V. Aksenova St. Petersburg State University, Physics Department, Ulyanovskaya St., 1, Petrodvorets, St. Petersburg, 198504 Russia. Tel.: +7 812 428 45 15; Fax: +7 812 428 72 40. E-mail: aksev@mail.ru

changes. This leads to a change in the limiting angle when the extraordinary ray starts to pass through the LC layer. This effect is of the threshold nature, the limiting angle and the penetration depth of light being dependent on the magnitude of the applied field. This study is aimed at investigation of the optical response of a 180° super-twist LC cell for various depths of penetration of the extraordinary ray into the layer.

2 Propagation of Light in a Chiral Medium

We consider a plane-parallel LC twist cell with the pitch P and thickness d . Let us introduce Cartesian coordinate system (x, y, z) with the z axis directed along a normal to the bounding planes, $0 \leq z \leq d$. We assume that the axis of the helix is directed along the z axis and the director $\mathbf{n}(\mathbf{r})$ is uniform in planes (x, y) :

$$\mathbf{n}(\mathbf{r}) \equiv \mathbf{n}(z) = (\cos \phi(z), \sin \phi(z), 0), \quad (2.1)$$

where $\phi(z) = q_0 z + \phi_0$, $q_0 = 2\pi/P$, and ϕ_0 is the initial phase.

The wave equation for the electromagnetic field in this medium has the form

$$(\text{rot rot} - k_0^2 \hat{\varepsilon}(z)) \mathbf{E}(\mathbf{r}) = 0, \quad (2.2)$$

where $\mathbf{E}(\mathbf{r})$ is the electric field, k_0 is the wave number in vacuum, $k_0 = 2\pi/\lambda$, λ is the wavelength and $\hat{\varepsilon}(z)$ is the permittivity tensor, which has the form [11]

$$\varepsilon_{\alpha\beta}(z) = \varepsilon_\perp \delta_{\alpha\beta} + \varepsilon_a n_\alpha(z) n_\beta(z), \quad (2.3)$$

where $\varepsilon_a = \varepsilon_\parallel - \varepsilon_\perp$; ε_\parallel and ε_\perp are the permittivities along and transverse to $\mathbf{n}(z)$, respectively.

In what follows we suppose that $P \gg \lambda$. In the geometrical optics approximation the solution of the wave equation (2.2) inside the medium has the form

$$\mathbf{E}(\mathbf{r}) = E_0(z) \mathbf{e}(z) \exp \left(i \mathbf{k}_\perp \cdot \mathbf{r}_\perp + i \int_0^z k_z(z') dz' \right), \quad (2.4)$$

where $E_0(z)$ is the local value of the amplitude, $\mathbf{e}(z)$ is the local vector of polarization, $\mathbf{k}(z) = (\mathbf{k}_\perp, k_z(z))$ is the wave vector.

For uniaxial permittivity tensor (2.3) and a fixed direction of the wave vector $\mathbf{t} = \mathbf{k}/k$ Eq. (2.2) in the first approximation has two well known solutions corresponding to the ordinary (o) and extraordinary (e) waves [12]:

$$k^{(o)} = k_0 n^{(o)}, \quad k^{(e)} = k_0 n^{(e)}. \quad (2.5)$$

Here, $n^{(o)}$ and $n^{(e)} = n^{(e)}(\mathbf{t})$ are the refractive indices for the ordinary and extraordinary rays, respectively,

$$n^{(o)} = \sqrt{\varepsilon_\perp}, \quad n^{(e)} = \sqrt{\frac{\varepsilon_\perp \varepsilon_\parallel}{\varepsilon_\parallel \cos^2 \theta + \varepsilon_\perp \sin^2 \theta}}, \quad (2.6)$$

where θ is the angle between the \mathbf{t} and \mathbf{n} vectors.

In our case the wave vectors \mathbf{k} and unit polarization vectors \mathbf{e} are functions of the coordinate z and the 2-D vector \mathbf{k}_\perp . We obtain from the Eq. (2.5)

$$k_z^{(o)}(\mathbf{k}_\perp, z) \equiv k_z^{(o)}(k_\perp) = \sqrt{\varepsilon_\perp k_0^2 - k_\perp^2} \quad (2.7)$$

for the ordinary wave and

$$k_z^{(e)}(\mathbf{k}_\perp, z) = \sqrt{\varepsilon_\parallel k_0^2 - k_\perp^2 - \frac{\varepsilon_a}{\varepsilon_\perp}(\mathbf{k}_\perp \cdot \mathbf{n}(z))^2} \quad (2.8)$$

for the extraordinary wave.

It is noteworthy that the transverse component of the wave vector \mathbf{k}_\perp is independent of z . If the axis x of the coordinate system (x, y, z) is chosen to lie along the fixed vector \mathbf{k}_\perp the \mathbf{t} vector takes the form $\mathbf{t}(z) = (\sin \chi(z), 0, \cos \chi(z))$, where $\chi(z)$ is the angle of the wave vector with the z axis. Then for the extraordinary wave we obtain from Eq. (2.5) $k_\perp = k_0 n^{(e)}(z) \sin \chi(z)$. Therefore the condition of the \mathbf{k}_\perp constancy corresponds to the conventional Snell equation

$$n^{(e)}(z) \sin \chi(z) = \text{const.} \quad (2.9)$$

Now we discuss the conditions under which light can propagate in a medium for the given \mathbf{k}_\perp , that is, for the given incidence angle. According to Eq. (2.7) the condition for propagation of the ordinary wave has the form $\sqrt{\varepsilon_\perp} k_0 \geq k_\perp$. Since the wave vector $\mathbf{k}^{(o)}$ is independent of z the wave will propagate rectilinearly in a medium throughout the region $0 \leq z \leq d$.

The conditions for propagation of the extraordinary wave are substantially different because the longitudinal component of the wave vector $k_z^{(e)}$ depends on z . According to Eq. (2.8), if the inequality

$$\varepsilon_\parallel k_0^2 - k_\perp^2 > \frac{\varepsilon_a}{\varepsilon_\perp} k_\perp^2 \cos^2 \phi(z) \quad (2.10)$$

is satisfied for all the angles $\phi(z)$ between the vectors \mathbf{k}_\perp and $\mathbf{n}(z)$, the extraordinary wave will propagate in a medium at any z . This condition corresponds to the inequality $k_\perp^2 < \min(\varepsilon_\perp, \varepsilon_\parallel) k_0^2$.

When the inverse inequality is satisfied for all angles $\phi(z)$ which corresponds to the condition $k_\perp^2 > \max(\varepsilon_\perp, \varepsilon_\parallel) k_0^2$, the wave will not propagate in a medium.

Finally in the case $\min(\varepsilon_\perp, \varepsilon_\parallel) k_0^2 \leq k_\perp^2 \leq \max(\varepsilon_\perp, \varepsilon_\parallel) k_0^2$, the intermediate situation occurs when the inequality (2.10) is satisfied only for a certain interval of angles $\phi(z)$. In this case there exists angle $\phi(z_t)$ at which the inequality (2.10) transforms to the equality. This corresponds to vanishing of the component $k_z^{(e)}$. With the further decrease of the angle $\phi(z)$ the component $k_z^{(e)}$ becomes imaginary and the wave begins to decay exponentially. Actually at this point the sign of $k_z^{(e)}$ changes and consequently the direction of the wave propagation along the z axis changes too. This means that point z_t is the turning point. In a certain sense, this effect is similar to the effect of the total reflection from some plane inside a medium.

It permits to derive the equation for the depth of the extraordinary wave penetration into the layer. Indeed the condition $k_z^{(e)}(\mathbf{k}_\perp, z) = 0$ gives

$$\cos^2 \phi(z_t) = \frac{\varepsilon_\perp}{\varepsilon_a} \left(\varepsilon_\parallel \frac{k_0^2}{k_\perp^2} - 1 \right) = 1 - \sin^2 \phi(z_t). \quad (2.11)$$

From here we get

$$z_t = \frac{P}{2\pi} \left[-\phi_0 \pm \arcsin \sqrt{\frac{\varepsilon_\parallel}{\varepsilon_a} \left(1 - \varepsilon_\perp \frac{k_0^2}{k_\perp^2} \right)} \right]. \quad (2.12)$$

For the ray incidence on plane $z = 0$, the minus sign should be taken in Eq. (2.12).

The electric field applied to the cell causes deformation of the helix. In this case it is convenient to express the director through the polar and azimuthal angles, θ and ϕ

$$\mathbf{n}(z) = (\cos \phi(z) \sin \theta(z), \sin \phi(z) \sin \theta(z), \cos \theta(z)). \quad (2.13)$$

Then the permittivity tensor (2.3) takes the form

$$\hat{\varepsilon}(z) = \begin{pmatrix} \varepsilon_\perp + \varepsilon_a \cos^2 \phi \sin^2 \theta & \varepsilon_a \cos \phi \sin \phi \sin^2 \theta & \varepsilon_a \cos \phi \sin \theta \cos \theta \\ \varepsilon_a \cos \phi \sin \phi \sin^2 \theta & \varepsilon_\perp + \varepsilon_a \sin^2 \phi \sin^2 \theta & \varepsilon_a \sin \phi \sin \theta \cos \theta \\ \varepsilon_a \cos \phi \sin \theta \cos \theta & \varepsilon_a \sin \phi \sin \theta \cos \theta & \varepsilon_\perp + \varepsilon_a \cos^2 \theta \end{pmatrix}. \quad (2.14)$$

In this case the wave vector component k_z of the ordinary wave is described by Eq. (2.7) as before. The appropriate equation for the extraordinary wave can be readily obtained in the form

$$k_{z\pm}^{(e)}(\mathbf{k}_\perp, z) = \frac{k_0}{\varepsilon_\perp + \varepsilon_a \cos^2 \theta} \left[-\sqrt{\varepsilon_\perp(1 - \alpha)} \varepsilon_a \sin \theta \cos \theta \cos \phi \right. \\ \left. \pm \varepsilon_\perp \sqrt{\varepsilon_\parallel \left(\alpha + \frac{\varepsilon_a}{\varepsilon_\perp} \cos^2 \theta \right) + (1 - \alpha) \varepsilon_a \sin^2 \theta \sin^2 \phi} \right], \quad (2.15)$$

where

$$\alpha = 1 - \frac{k_\perp^2}{k_0^2 \varepsilon_\perp}.$$

In this case the condition $k_{z+}^{(e)} = k_{z-}^{(e)}$ corresponds to the turning point, that is,

$$\sqrt{\varepsilon_\parallel \left(\alpha + \frac{\varepsilon_a}{\varepsilon_\perp} \cos^2 \theta \right) + (1 - \alpha) \varepsilon_a \sin^2 \theta \sin^2 \phi} = 0 \quad (2.16)$$

and the component $k_z^{(e)}$ is equal to

$$k_z^{(e)} = \frac{k_\perp}{\varepsilon_\perp + \varepsilon_a \cos^2 \theta} \varepsilon_a \sin \theta \cos \theta \cos \phi.$$

It should be noted that in the absence of the external field $k_z^{(e)} = 0$. When the external field is applied $k_z^{(e)}$ is not equal to zero at the turning point for the oblique director (Eq. (2.13)). In fact the ray or the Poynting vector is related to the energy transfer. So the z component of the ray vector should reduce to zero at the turning point rather than the component k_z of

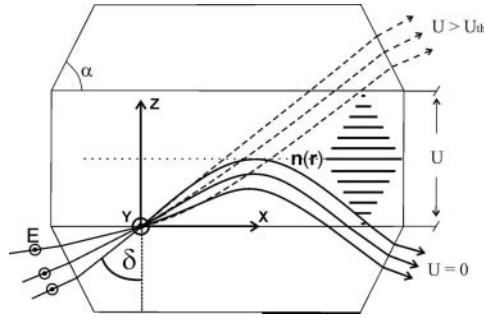


Figure 1. Liquid crystal cell consisting of two trapezoidal glass prisms and LC layer. Extraordinary ray trajectories: in the absence (solid lines) and presence (dashed lines) of the electric field. Here $\mathbf{n}(\mathbf{r})$ is the director; α is the base angle of the prisms; δ is the angle of incidence of light on the layer; \mathbf{E} is the vector of the electric field in the incident light; (x, y, z) is the Cartesian coordinate system; U is the control voltage; U_{th} is the threshold voltage.

the wave vector. The Poynting vector \mathbf{S} which defines the direction of the ray propagation is connected to the wave vector through the relation

$$\mathbf{S} \sim \hat{\epsilon} \mathbf{R} \mathbf{k}.$$

If the tensor $\hat{\epsilon}$ is used in the explicit form (2.14) it can be readily seen that $S_z = 0$ in the turning point. Physically this corresponds to the turn back of the ray, that is, to the internal reflection.

As a result the extraordinary rays that are reflected inside an LC layer in the absence of the electric field will pass through the cell in the presence of the electric field which is in excess of the Freedericksz threshold (Fig. 1).

3 Experimental Results

The effect of an alternating electric field on the trajectory of an extraordinary ray in a 180° super-twist LC cell was studied for various depths of the extraordinary ray penetration into a layer using the experimental setup presented in Fig. 2. A He-Ne laser (L) was used as a source of polarized radiation at wavelength $\lambda = 632.8$ nm emitted in a beam of 1 mm diameter. The beam passed through a half-wave plate $\lambda/2$ which provided the necessary polarization of the wave and was incident on the entrance face of an LC cell. The direction of polarization of the laser beam coincided with that of the LC director at the layer boundary. The cell was placed on a rotation stage with an angle measuring device which allowed

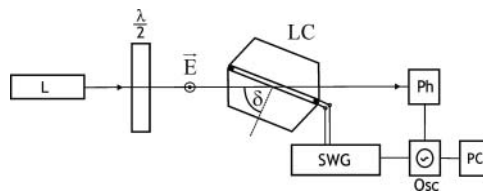


Figure 2. Experimental setup. L: laser; $\lambda/2$: half-wave plate; LC: liquid crystal cell; Ph: photodetector; SWG: sine wave voltage generator; Osc: digital oscilloscope; PC: computer.

us to vary the angle of the light incidence on the layer. The angle of incidence on the entrance face of the glass prism was recalculated into the angle of incidence on the LC layer. The radiation intensity was measured by a photodetector (Ph). Optical and control electric signals were recorded by a two-channel digital oscilloscope (Osc). As a source of a control signal, we used a sine wave voltage generator (SWG), which produced voltage pulses up to 30 V_{rms} with the duration 0.1–5 s and the carrier frequency f from 20 Hz to 20 kHz.

The LC cell consisted of two trapezoidal glass prisms made of optical glass with the refractive index $n_g = 1.7002$ and having the base angles $\alpha = 68.0^\circ$. The 18 μm LC layer was placed between the prisms. Transparent current-conductive electrodes were deposited on the glass surfaces bounding the LC. The planar orientation of the director on the surface of the electrodes, which is orthogonal to the plane of the figure, was created by rubbing the polyimide coatings in the same directions. The angle of the director with the surface of the LC layer, determined by the polarimetric method, was 2° [13]. For measurements we used an LC mixture consisting of nematic LC 1466 (NIOPIK, Russia) with a 0.2 wt.% chiral dopant VICH-3 (Vilnius University, Lithuania). The mixture showed positive dielectric anisotropy and its refractive indices were $n_e = 1.691$ and $n_o = 1.551$. The pitch was determined by the Cano-Grandjean method and was equal to 32 μm . At the layer thickness $d = 18 \mu\text{m}$, the director at one layer interface was turned by 180° with respect to that at the other interface.

In the above geometry, $\phi_0 = -\pi/2$, $d = P/2$. At the given angle of incidence on the glass-LC interface, δ , it follows from the Snell law that

$$k_0 n_g \sin \delta = k_\perp.$$

Then the depth of the ray penetration into LC (2.12) can be written in the form

$$z_t = \frac{d}{2} - \frac{d}{\pi} \arcsin \sqrt{\frac{\varepsilon_\parallel}{\varepsilon_a} \left(1 - \frac{\varepsilon_\perp}{n_g^2 \sin^2 \delta} \right)}. \quad (3.1)$$

When the angle of the extraordinary wave incidence on the glass-LC interface, δ , varies from $\delta_o = \arcsin(n_o/n_g)$ to $\delta_e = \arcsin(n_e/n_g)$, the coordinate of the point of the ray reflection inside the LC layer shifts from the middle of the layer to the glass-LC interface according to Eq. (3.1). Here, $n_o = \sqrt{\varepsilon_\perp}$ and $n_e = \sqrt{\varepsilon_\parallel}$.

In our experiment the angles of the ray incidence on the layer varied within the range 62.8° to 79.7° , whereby the depth of the ray penetration into the layer varied from 8.7 to 1.7 μm (Fig. 3).

The threshold voltages for various angles of light incidence on the LC were determined using the setup depicted in Fig. 2. The voltages were found from the voltage dependences of the intensity of light transmitted through the cell. The threshold voltage corresponded to the transmission at a level of 10% of the maximum intensity of the transmitted light. It was found out that the threshold voltage U_{th} increased with the incidence angle, i.e., as the depth of the ray penetration into the LC layer in the absence of an external field decreased according to Eq. (3.1). Under our experimental conditions, the value of U_{th} varied within 1.32 to 3.80 V_{rms} as the depth of penetration z_t varied from 8.7 to 1.7 μm (Fig. 1). This is due to the fact that, to deflect the LC director oriented by the solid surface at the same angle near the surface and in the middle of the layer, different voltages are necessary, the voltage near the surface being higher than that in the middle [7].

The local dynamics of the director reorientation at various distances from the interface was studied by the optical responses of the cell when the control voltage pulses were

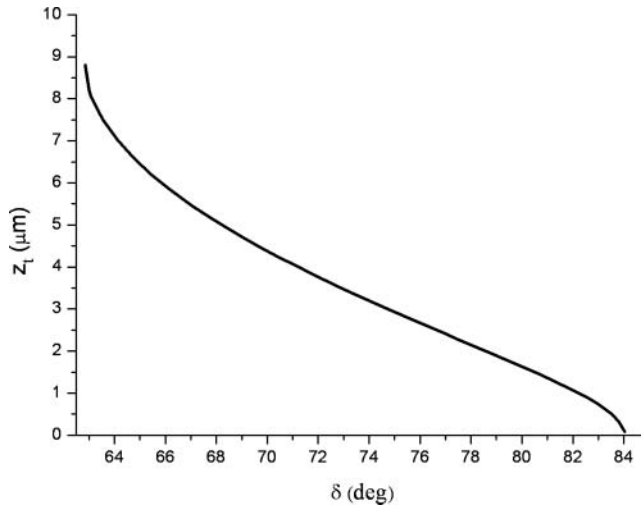


Figure 3. Depth of the extraordinary ray penetration z_l into the LC layer as a function of the incidence angle δ .

applied. The control voltage was chosen to be higher than the threshold voltage $3.80 V_{\text{rms}}$ for all the penetration depths. In our experiments the control voltage was varied within 4.00 to $6.00 V_{\text{rms}}$, which opened the cell completely for all the penetration depths.

Oscillograms of the optical responses of the cell as functions of the depth of the ray penetration into the LC layer at voltage $U = 5.00 V_{\text{rms}}$ are shown in Fig. 4 (for the electric

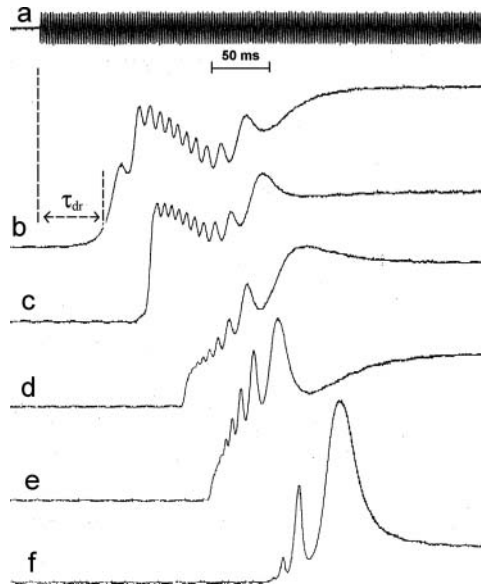


Figure 4. Optical response of the LC cell after electric field was switched on, $U = 5.00 V_{\text{rms}}$, $f = 1000 \text{ Hz}$. For this frequency the dielectric anisotropy is equal to 117. a — control voltage pulse, b, c, d, e, f — optical responses for $z_l = 8.7, 7.4, 5.1, 3.0, 1.7 \mu\text{m}$.

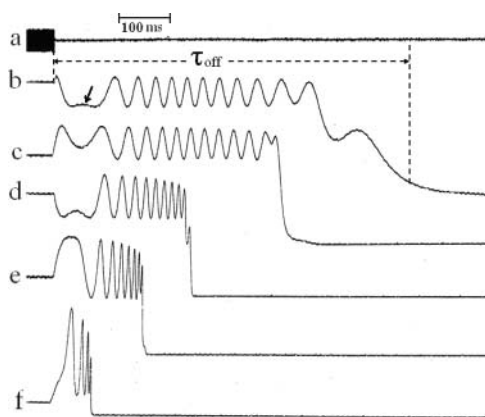


Figure 5. Optical response of the LC cell with electric field was switched off, $U = 5.00 \text{ V}_{\text{rms}}$, $f = 1000 \text{ Hz}$. a — control voltage pulse, b, c, d, e, f — optical responses for $z_t = 8.7, 7.4, 5.1, 3.0$, and $1.7 \text{ } \mu\text{m}$, respectively.

field switched on) and Fig. 5 (for the electric field switched off). It should be noted that the intensity variation curves for the field switched on and off undergo clearly exhibited oscillations.

The intensity oscillations can be explained by the fact that the extraordinary wave passing through the cell partially reflects from the LC-glass interfaces, the reflected waves interfere, and the phase difference between them changes during reorientation of the director. Moreover, the monotonic behavior of the phase difference in the interfering waves breaks down (arrow in Fig. 5). This breaking can be explained by the arising LC backflow [14].

The delay time τ_{dr} of the effect onset can be readily determined from the oscillograms of the intensity increasing of the transmitted light (Fig. 4). These times are found for

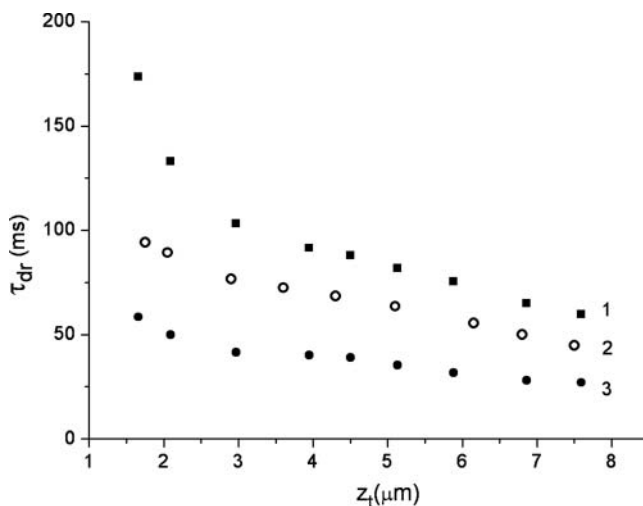


Figure 6. Delay time of the signal rise, τ_{dr} as a function of the distance from the layer boundary z_t for different control voltages $U = 4.00 \text{ V}_{\text{rms}}$ (1); $U = 5.00 \text{ V}_{\text{rms}}$ (2); $U = 6.00 \text{ V}_{\text{rms}}$ (3).

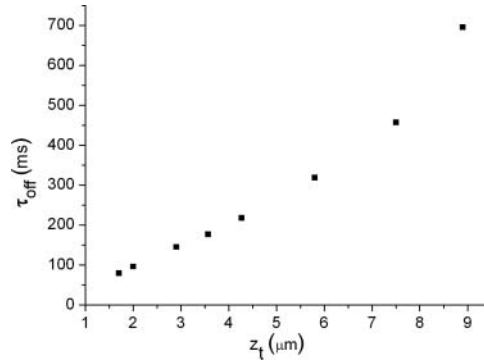


Figure 7. Turn-off time τ_{off} as a function of the distance from the layer boundary z_t .

various angles of incidence δ and various voltages. Using Eq. (3.1) angles of incidence δ are recalculated to the penetration depths z_t . The delay time dependence on the penetration depth is shown in Fig. 6 for several values of the control voltage. It can be seen from Fig. 6 that at a same voltage the delay time decreases as the depth of the ray penetration into the layer increases. In order to the light transmittance through the cell takes place the director should turn in the layer $z \sim z_t$. Since near the boundary reorientation of the director is difficult due to the anchoring with the orienting surface [15] delay time near the surface will be greater than in the depth of the cell. Thus, τ_{dr} decreases with increasing z_t as it is shown in Fig. 6.

The turn-off time of the effect, τ_{off} , was determined from the optical responses obtained for various depths of the ray penetration into the layer. The turn-off time can be interpreted as a recovery time of the initial configuration of the director. Figure 7 shows the turn-off time τ_{off} as a function of the penetration depth z_t . It can be seen from Fig. 7 that τ_{off} decreases with a decrease in z_t . This dependence can be qualitatively explained by the fact that the rate of the recovery of the initial configuration is proportional to the elastic torque acting on the director [15], which is larger near the surface.

4 Conclusions

In our study we determined the threshold voltages for the refraction disturbance effect. It has been found that the threshold value increases as the depth of the light penetration decreases. We determined the delay times of the onset of the refraction disturbance effect at various distances from the layer boundary for various values of the control voltages, as well as the times of recovery of the initial director configuration for the same light penetration depths. Thus, it has been demonstrated that the used experimental technique provides investigation of the dynamics of the local reorientation of the director at various distances from the glass-LC interface.

Acknowledgements

This study was supported by St. Petersburg State University, grant 11.38.45.2011.

References

- [1] Freedericksz, V., & Zwetkoff, V. (1934). *Physikalische Zeitschrift der Sowjetunion*, 6, 5.
- [2] Simoni, F., Bloisi, F., Vicari, L., Warenghem, M., Ismaili, M., & Hector, D. (1993). *Europhys. Lett.*, 21, 189.
- [3] Warenghem, M., Louvergneux, D., & Simoni, F. (1996). *Mol. Cryst. Liq. Cryst.*, 282, 235.
- [4] Rayes, J. A., & Rodriguez, R. F. (1998). *Mol. Cryst. Liq. Cryst.*, 317, 135.
- [5] Olivares, J. A., Rodriguez, R. F., & Rayes, J. A. (2003). *Opt. Comm.*, 221, 223.
- [6] Mendoza, C. I., Olivares, J. A., & Rayes, J. A. (2004). *Phys. Rev. E*, 70, 062701.
- [7] Mendoza, C. I., & Rayes, J. A. (2006). *Appl. Phys. Lett.*, 89, 091912.
- [8] Aksenova, E. V., Karetnikov, A. A., Kovshik, A. P., Romanov, V. P., & Val'kov, A. Yu (2005). *Europhys. Lett.*, 69, 68.
- [9] Aksenova, E. V., Karetnikov, A. A., Kovshik, A. P., Kryukov, E. V., & Romanov, V. P. (2008). *J. Opt. Soc. Am. A*, 25(3), 600.
- [10] Karetnikov, A. A., Karetnikov, N. A., Kovshik, A. P., Ryumtsev, E. I., Aksenova, E. V., Kryukov, E. V., & Romanov, V. P. (2010). *Opt. Spectr.*, 108, 947.
- [11] de Gennes, P. G. & Prost, J. (1993). *The Physics of Liquid Crystals*, Clarendon Press: Oxford, UK.
- [12] Landau, L. D., Lifshitz, E. M., & Pitaevsky, L. P. (1995). *Electrodynamics of Continuous Media*, Butterworth-Heinemann: Oxford, UK.
- [13] Karetnikov, A. A., Karetnikov, N. A., Kovshik, A. P., & Ryumtsev, E. I. (2007). *Opt. Spectr.*, 103(4), 646.
- [14] Shen, S.-H. & Yang, C.-L. (2002). *Appl. Phys. Lett.*, 80, 3721.
- [15] Blinov, L. M. (1983). *Electro-Optical and Magneto-Optical Properties of Liquid Crystals*, Wiley: New York, USA.